Molecular Dynamics with a Quantum-Chemical Potential: Solvent Effects on an S_N2 Reaction at Nitrogen

Haiyan Liu, Florian Müller-Plathe and Wilfred F. van Gunsteren*

Abstract: Solvent effects on an S_N2 reaction at nitrogen ($Cl^- + NH_2Cl \rightarrow ClNH_2 + Cl^-$) in dimethyl ether solution were studied by means of molecular dynamics simulation with a combined quantum-chemical and molecular-mechanical potential. The energetics and geometrical parameters of the reaction in the gas phase, calculated by means of the semiempirical model PM3 (the quantum chemical part of the combined potential), were compared with ab initio calculations up to the 6-311+G**/MP2 and 6-311+G(2d,p)/MP2 levels of theory. Compared with the gas phase potential energy surface, the free energy profile of the reaction in dimethyl ether solution shows that the solvent makes the ion–dipole complex well shallower by approximately 6.4 kcal mol^{-1} and raises the height of the effective barrier from the complex to the transition state by about 2.2 kcal mol^{-1}. The overall transition barrier between the separated reactants and the products is raised from 6.4 kcal mol^{-1} to 15.0 kcal mol^{-1} upon solvation. The radial distribution functions between solvent–solute atom pairs at different stages of the reaction course were compared. Results show that better solvation of the charge-localised separated reactants is responsible for the increase in the barrier height. Polarisation of the solute by its surroundings is also discussed.

Keywords
computer simulations · molecular dynamics · nucleophilic substitutions · quantum chemistry · solvent effects

Introduction

While quantum-chemical methods can provide excellent descriptions of molecular systems in the gas phase (in a vacuum), they often fail to account for effects caused by an environment, such as a solvent, a surface or the active site of a protein. This happens because explicit treatment of all the atoms that form the environment quickly becomes prohibitively expensive as the size of the system increases. On the other hand, classical molecular simulation methods based on empirical force fields have the capability to treat effects of the environment, of finite temperature as well as dynamic processes, and so on. However, since the force fields are empirical, they can be inaccurate and they may fail in circumstances for which they have not been designed or parameterised. One of the classic cases is the breaking and making of chemical bonds, their description not being included in standard force fields.

The approach used in this article combines the best of both worlds in order to study a chemical reaction in solution. We use a hybrid scheme in which the reactants and the products are treated by quantum chemistry, whereas the solvent is described by a classical force field.[1] This hybrid method allows us to study the evolution of the system over several hundred picoseconds by conventional molecular dynamics (MD) with the forces on the reactant atoms being evaluated by quantum chemistry. We have used this hybrid approach previously on the conformational equilibrium of dimethoxyethane in solution.[1d] There, it was successful: it explained features that could not be explained by vacuum quantum chemistry nor by a continuum reaction field approach.[2] Details of the method are reported elsewhere.[1]

In this paper, we investigate the model reaction (1) in the gas phase and in solvent (dimethyl ether, DME). We use con-

$$Cl^- + NH_2Cl \longrightarrow ClNH_2 + Cl^- \quad (1)$$

ventional ab initio quantum chemistry to calibrate the semiempirical method (PM3[3]) in a vacuum, which we then use in the hybrid MD scheme in solution. We report properties of statistical-mechanical nature (for example the free energy profile along the reaction coordinate) as well as electronic properties, reflecting the dual origins of the method.

Experimental and theoretical investigations have suggested an S_N2 mechanism for nucleophilic substitutions at nitrogen;[4, 5] double labelling experiments with isotopes have yielded evidence for a classical S_N2 transition state.[4] Gas phase ab initio quantum-mechanical calculations have been reported for the model reaction (2)[5] which show the same characteristics

$$F^- + NH_2F \longrightarrow FNH_2 + F^- \quad (2)$$

as S_N2 reactions at carbon,[6] namely, formation of a complex and a symmetric transition state (barrier height = 24.0 kcal mol^{-1} at the TZP+/CISD level of theory). S_N2 reactions at carbon in the gas phase and in solution have been

[*] W. F. van Gunsteren, H. Liu, F. Müller-Plathe
Laboratorium für Physikalische Chemie, Eidgenössische Technische Hochschule
ETH-Zentrum, CH-8092 Zürich (Switzerland)
Telefax: Int. code + (1) 632-1039
e-mail: wfvgn@igc.chem.ethz.ch

  0947-6539/96/0202-0191 $ 10.00+.25/0

studied extensively.[6, 7, 8] It has been found that in solution the reactants are better stabilised by polar, protic solvents than the transition state, the charges on which are less localised.[6a] It has yet to be shown to what extent these findings apply to S_N2 reactions at nitrogen.

Results and Discussion

Ab initio calculations were carried out at the SCF/6-31+G**, SCF/6-311+G** and MP2/6-311+G** levels of theory. The resulting geometrical parameters and relative energies for structures shown in Scheme 1 are listed in Table 1.

Harmonic vibrational frequencies calculated at SCF/6-31+G** level show that complex **1** (with C_S symmetry) is actually a transition state for the migration of Cl^- between the two hydrogen atoms, with an imaginary frequency of 133i cm^{-1}. This is quite similar to the $F^- \cdots NH_2F$ complex with the same symmetry.[5b] The transition state of the S_N2 reaction has an imaginary frequency of 474i cm^{-1}.

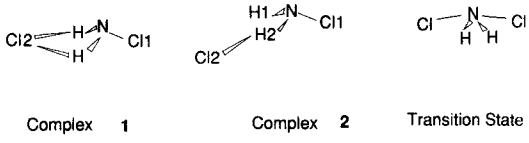

Complex 1 Complex 2 Transition State

Scheme 1. Different $NH_2Cl_2^-$ species.

Table 1. Gas phase optimised geometrical parameters and relative energies of different $NH_2Cl_2^-$ species (Scheme 1) at different levels of theory [a].

	PM3	SCF/ 6-31+G**	SCF/ 6-311+G**	MP2/ 6-311+G**[b]
$NH_2Cl + Cl^-$, separated reactants				
r_{N-Cl}	1.737	1.726	1.730	1.746
r_{N-H}	0.997	1.001	1.001	1.018
∢Cl-N-H	108.6	106.2	105.8	105.5
∢H-N-H	109.7	108.1	107.6	105.8
energy	0	0	0	0 (0)
Complex **1**				
r_{N-Cl1}	1.753	1.748	1.749	1.760
r_{N-H}	1.004	1.004	1.004	1.022
r_{Cl2-H}	2.449	2.789	2.799	2.631
∢Cl1-N-H	107.9	105.4	105.2	105.4
∢H-N-H	107.6	102.2	102.1	98.7
∢Cl2-H-N	106.9	111.6	111.7	112.2
∢Cl1-N-Cl2	120.3	126.0	126.0	126.0
energy	−15.4	−13.2	−13.2	−15.2 (−15.5)
Complex **2**				
r_{N-Cl1}	1.750	1.745	1.747	1.757
r_{N-H1}	0.997	1.002	1.002	1.019
r_{N-H2}	1.065	1.012	1.012	1.041
r_{Cl2-H2}	1.739	2.405	2.399	2.141
∢H1-N-H2	108.2	104.1	103.8	102.5
∢N-H2-Cl2	164.5	150.1	150.2	163.4
∢Cl1-N-H1	106.0	104.4	104.1	103.5
∢Cl1-N-H2	110.3	106.2	106.1	105.9
$T_{Cl2-H2-N-Cl1}$	121.0	128.7	129.4	130.5
energy	−18.9	−13.5	−13.5	−16.6 (−16.6)
Transition state				
r_{N-Cl}	2.006	2.288	2.288	2.220
r_{N-H}	0.992	1.000	1.000	1.019
∢Cl-N-Cl	173.2	166.2	166.4	170.2
∢H-N-H	113.4	106.9	106.0	103.3
∢Cl-N-H	91.9	85.9	85.9	86.9
energy	6.4	9.5	9.6	3.3 (2.8)

[a] Distances in Å; angles in °; energies in kcal mol^{-1}. [b] Energies calculated at MP2/6-311+G** geometries, but at the MP2/6-311+G(2d,p) level, are given in parentheses.

The results in Table 1 do not show strong dependence on the levels of theory used. At the SCF level, going from the 6-31+G** basis set to the 6-311+G** basis set has only minor effects on the resulting geometrical parameters. The relative energies show almost no change (less than 0.1 kcal mol^{-1}). Inclusion of electron correlation at the MP2 level has a somewhat larger effect. Inclusion of a second polarisation function on the heavy atoms [MP2/6-311+G(2d,p)] has no significant effect on the gas-phase energetics (Table 1). This insensitivity to change in basis set also indicates that the effect of the basis set superposition error is minor. Most of the geometrical parameters show only moderate changes, except that the Cl–H distances in the two hydrogen-bonded complexes are shortened by more than 0.1 Å. The transition state is stabilised by approximately 6 kcal mol^{-1} compared with the SCF result with the same basis set, while complex **1** and complex **2** are stabilised by approximately 2 kcal mol^{-1} and 3 kcal mol^{-1}, respectively. Similar effects have also been found in the study of reaction (2), in which the configuration interaction method has been used to deal with electron correlation.[5] At the highest level of theory employed, that is, the MP2/6-311+G** level, the "intrinsic" barrier of reaction (1), namely, the energy difference between the transition state and complex **2**, is 19.8 kcal mol^{-1}, higher than that of the analogous reaction (3) (13.9 kcal mol^{-1} calculated at the

$$Cl^- + CH_3Cl^- \longrightarrow ClCH_3 + Cl^- \quad (3)$$

MP2/6-31G* level[6a, 9]). The difference between the barrier heights of these two reactions involving chloride is almost equal to that between the barrier heights of the two reactions involving fluoride, reaction (2) (24.0 kcal mol^{-1} at the TZP+/CISD level[5]) and reaction (4) (17.1 kcal mol^{-1} at the DZDP/CISD level).[5] (For a more recent discussion, see ref. [7].) Both cases

$$F^- + CH_3F \longrightarrow FCH_3 + F^- \quad (4)$$

suggest that the S_N2 mechanism is viable for nucleophilic substitution at nitrogen, although the barriers may be higher than those of analogous S_N2 reactions at carbon.

The ability of the PM3 method, the quantum-chemical model used in our hybrid scheme, to describe reaction (1) can be judged by comparing it with ab initio models. Most of the geometrical parameters and relative energies agree reasonably well between PM3 and MP2 (Table 1). However, there are also some discrepancies. Complex **1** becomes a real minimum rather than a saddle point, the lowest mode having a frequency of 75 cm^{-1}. This complex, however, was not observed in the MD simulations since its energy is about 6 k_BT higher than that of complex **2**. The height of the intrinsic barrier is overestimated by approximately 5.4 kcal mol^{-1} compared with the MP2/6-311+G** results. Notable discrepancies in the geometrical parameters are the Cl–H "hydrogen bond" distances in the two complexes, for which the PM3 results deviate slightly more from the MP2 results than the ab initio SCF results, albeit with opposite sign. Another large deviation (0.2 Å) occurs in the N–Cl distance of the transition state. In the transition state, the Cl-N-Cl angle calculated by PM3 also bends in the opposite direction with respect to that shown in Scheme 1, although it still remains close to 180°. However, in general, the PM3 model is able to reproduce the basic features of this reaction in the gas phase and thus should be appropriate for MD simulations of the reaction in DME solution.

0947-6539/96/0202-0192 $ 10.00+.25/0 Chem. Eur. J. 1996, 2, No. 2

The free energy profile along the reaction coordinate of the reaction in solution at 248 K and 1 atm has been determined by means of MD simulations and umbrella sampling[10] (see computational details). The reaction coordinate r_c has been defined as the difference between the two N–Cl distances of the solute. It has large values when the reactants are separated. At the transition state, its value is 0.

The calculated free energy profile is shown in Figure 1, together with the gas-phase potential energy curve along the minimum energy reaction path calculated by PM3. The reaction

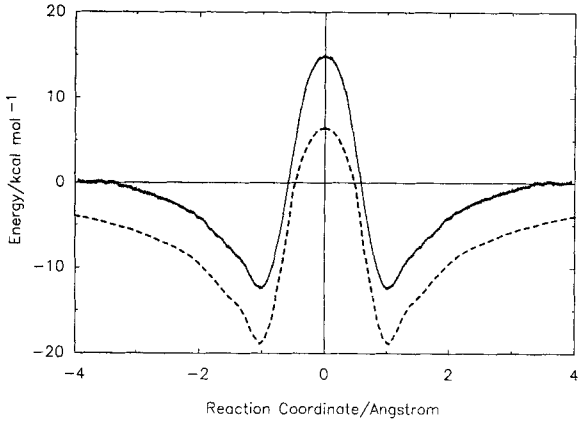

Fig. 1. Free energy profile for the S_N2 reaction $Cl^- + NH_2Cl \rightarrow ClNH_2 + Cl^-$ in dimethyl ether solution (solid line) and the gas-phase potential energy surface (calculated by PM3, dashed line). In both curves, the energies of the separated reactants are taken to be zero. The reaction coordinate is the difference between the two Cl–N distances.

path from the intermediate (complex **2**) to the transition state is as follows. As the Cl2 atom approaches the nitrogen atom, the H-N-H plane becomes more and more perpendicular to the N–Cl1 vector until the transition state is reached. Meanwhile, the Cl2 atom gets closer to the plane which corresponds to the symmetry plane of complex **1**. C_s symmetry is reached only when r_c becomes less than 0.3 Å. As in the analogous carbon reactions, an inversion of the tetrahedral configuration (in this case, formed by the N atom, its lone-pair electrons and the two H atoms) happens in going from the reactant to the product state. The overall features of the two profiles in Figure 1 are quite similar, suggesting a similar reaction path in solution and in the gas phase. Inspection of the solute configurations encountered during the MD simulations confirmed that, in solution, the basic features of the reaction path remain the same as in the gas phase. The intermediate complex corresponds to complex **2**.

The effects of solvation on the relative free energies are moderate. The well depth at the intermediate complex minimum (complex **2**) decreased from 18.9 to 12.5 kcal mol^{-1} (relative to the separated reactants both in the gas phase and in solution). The transition state barrier is raised from 6.4 to 15.0 kcal mol^{-1}. The largest part of the solvent effect (ca. 6 kcal mol^{-1}) occurs during the process of complex formation, owing to the superior solvation of the separated species compared with the complex. As in the well-studied carbon case (reaction (3)),[6b] one can expect that a solvent with stronger anion–solvent interactions will further decrease the well depth. However, for this reaction, a solvent with much stronger anion–solvent interactions may be needed to change the mechanism into a "concerted" S_N2 one, that is, to make the complex well in the free energy profile disappear completely and the free energy profile unimodal, since the well in the gas-phase energy profile is much deeper than for the carbon analogue. The "intrinsic" barrier was increased by approximately 2 kcal mol^{-1} in DME solution, reflecting the difference between the ability of DME to solvate the transition state and to solvate the more charge-localised hydrogen-bonded complex. In Figure 1, one also observes the effective shielding of the charge–dipole interaction between Cl^- and NH_2Cl at intermediate distances: in solution, the "infinite-separation" limit is reached for an r_c of approximately 4 Å (the corresponding Cl–N distance is about 5.7 Å).

Solute–solvent atom-pair distribution functions have been computed from the MD trajectories. These functions, which correspond to the separated-reactant state, the hydrogen-bonded complex state (complex **2**) and the transition state, respectively, are shown in Figure 2. Comparing the distribution functions of different states, it is seen that the rearrangement of the solvent molecules during the reaction process is consistent with the direction of charge transfer. Key changes occur around the Cl atoms. From the reactant state to the transition state, negative charge is transferred from the attacking Cl^- anion to the departing Cl atom. Correspondingly, in the Cl–C pair distribution functions (Figs. 2a and b), the peak at about 4 Å around the Cl^- anion decreases, while the same peak around the attached Cl atom is narrowed. The peak at about 5.2 Å in the curves for the Cl–O pairs (Figs. 2c and d) shows the same trend. However, the peaks are not high compared with, for example, those in the case of Cl^- in protic solvent,[6] and their changes are moderate. This is because of the large size and the moderate partial charges of the solvent atoms, and explains why the free energies of solvation of complex **2** and the transition state differ by only about 2 kcal mol^{-1}.

Atom-pair distribution functions involving solute atoms other than the two Cl atoms are far less structured (Figs. 2e and f), but they still reflect the changes in charge distribution and in structure of the solute. For example, a small peak at about 3.0 Å appears in the N–O pair distribution function for the separated-reactant state (Fig. 2f), suggesting the existence of weak hydrogen bonds. This peak disappears as the negatively charged Cl^- anion approaches the nitrogen in the complex **2** state. The existence of these weak hydrogen bonds also explains why in Figure 2c the first peak in the curve corresponding to the separated state shows a shoulder at a smaller Cl–O distance. The differences between the radial distribution functions around the two solute hydrogen atoms for the complex **2** state (not shown here) are consistent with the fact that only one of the hydrogen atoms is hydrogen-bonded to the Cl^-.

Upon solvation, the solute is polarised. This is reflected in the difference between its charge distributions in the gas phase and in solution. Figure 3 shows the Mulliken charges on solute atoms as a function of the reaction coordinate. The curves corresponding to the reaction in solution show the same characteristic charge transfers as those of the gas-phase reaction. In both cases, the charges on the two solute hydrogen atoms are different in between $r_c = 0.3$ and 1.3 Å, corresponding to the asymmetric hydrogen-bonded complex **2** in Scheme 1. However, the polarisation of the solute is also clearly shown in Figure 3. From the separated reactants up to an r_c of about 0.5 Å, the Mulliken charge on the nitrogen atom is about 0.1 e more negative for the reaction in solution. At the same time, the two solute hydrogen atoms are more positively charged. In the transition state, the polarisation of the solute is somewhat less obvious. The negative charges on the two Cl atoms are slightly larger in solution than in the gas phase, while the positive charge on the nitrogen is smaller and the positive charges on the two hydrogen atoms are larger than their gas-phase values. For this reaction, DME as a solvent has only slightly modified the charge-transfer process.

  0947-6539/96/0202-0193 $ 10.00+.25/0

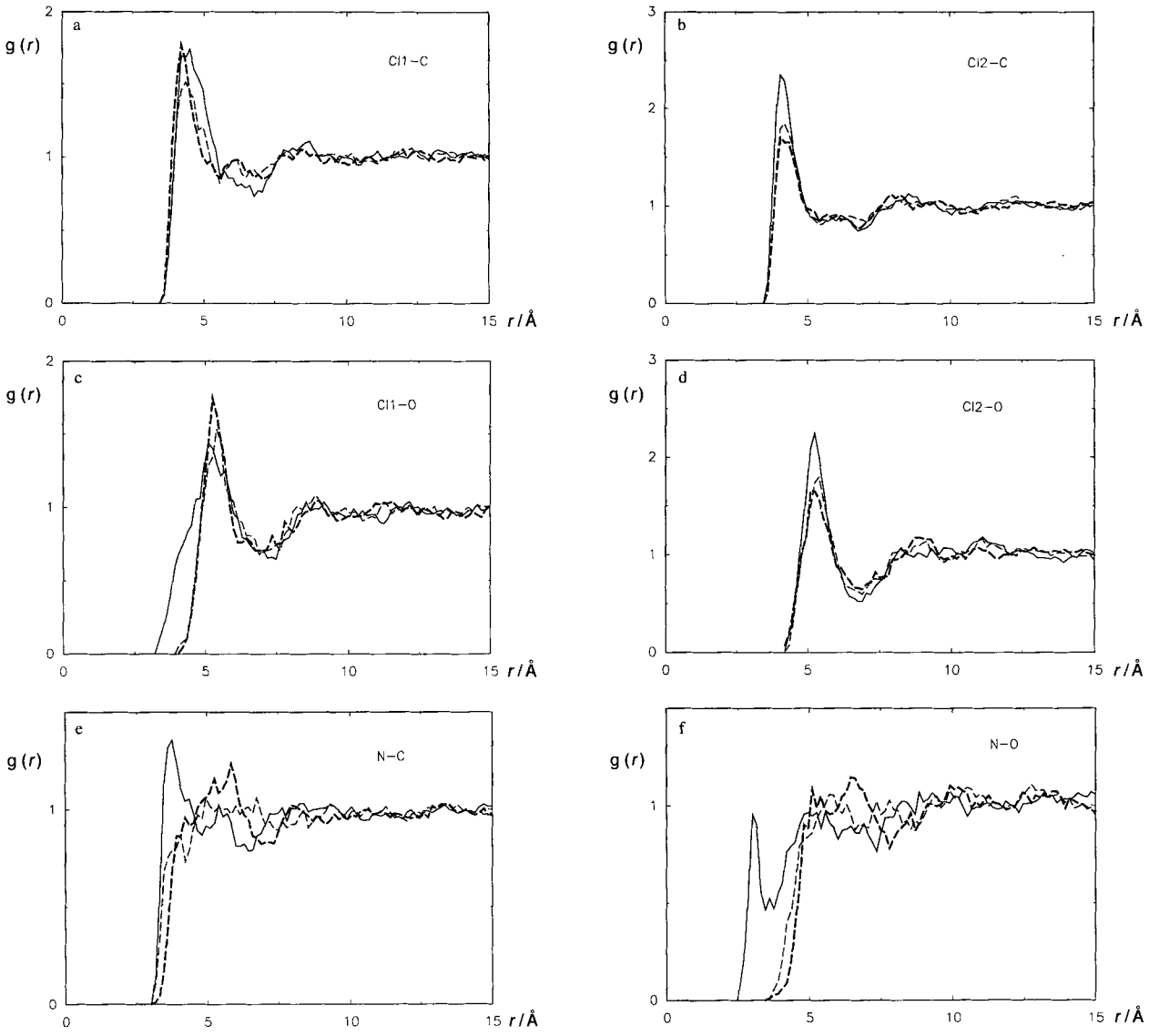

Fig. 2. Solute–solvent atom-pair distribution functions in the separated-reactants state (solid lines), the ion–molecule complex **2** state (dashed lines) and the transition state (thick dashed lines) for the S_N2 reaction $Cl^- + NH_2Cl \rightarrow ClNH_2 + Cl^-$ in dimethyl ether solution. a) Cl1–C pairs. b) Cl2–C pairs. c) Cl1–O pairs. d) Cl2–O pairs. e) N–C pairs. f) N–O pairs. Cl1 is the attached Cl atom; Cl2 is the attacking Cl atom.

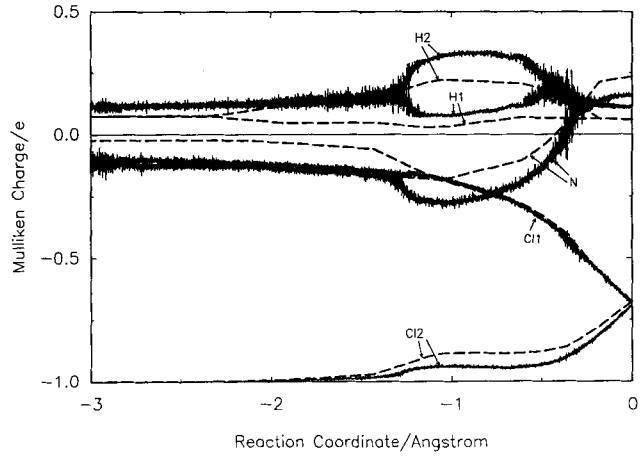

Fig. 3. Mulliken charges (PM3) on atoms along the reaction coordinate of the S_N2 reaction $Cl^- + NH_2Cl \rightarrow ClNH_2 + Cl^-$ in the gas phase (dashed lines) and in dimethyl ether solution (solid lines). The reaction coordinate is the difference between the two Cl–N distances. Cl1 is the attached Cl atom; Cl2 is the attacking Cl atom; H2 is the H atom forming a hydrogen bond with Cl2.

The transfer of negative charge to the attached Cl atom is almost unchanged. The negative charge on the Cl^- in the complex state is increased by about 0.06 e. Consequently, its decrease is slightly accelerated when the system goes from the complex state to the transition state.

Conclusion

To summarise, results obtained with the hybrid MD scheme show that in a dipolar solvent, the barrier height of reaction (1) is raised because solvent molecules interact more strongly with the reactants. In dimethyl ether solution, the barrier height is only moderately increased. One major reason for this is that DME is aprotic and in our solvent model the partial charge on the methyl groups is small (0.18 e). In the hybrid scheme, the wavefunction of the solute electrons responds to the change in the solvent charge distribution and thus the polarisation of the solute is taken into account naturally. Polarisation effects are observed in these simulations; this provides further support for the use of hybrid quantum-classical simulation methods in studying chemical processes in solution.

0947-6539/96/0202-0194 $ 10.00+.25/0 Chem. Eur. J. 1996, 2, No. 2

Computational Details

The combined quantum-mechanical and molecular mechanical potential energy function used here contains various Lennard-Jones terms and Coulombic terms [1 d]. Parameters for these terms have been taken from the GROMOS force field [11] and are listed in Table 2. The DME molecules were held rigid by the SHAKE method [12]. The heat of vaporisation and the density of liquid DME at 248 K and 1 atm calculated from MD simulation with this DME model have been found to be in good agreement with experimental values. A truncated-octahedron periodic box containing one $NH_2Cl_2^-$ as solute and 349 DME molecules as solvent was used. The cutoff radius for the nonbonded interactions was 11 Å. The weak coupling method [13] was used to keep the temperature at 248 K and the pressure at 1 atm with relaxation times of 0.1 and 0.3 ps, respectively. The initial structure of the solute was the gas-phase transition state structure optimised by PM 3. The length of the time steps was 0.5 fs. The restraining potential energy function used in the umbrella sampling procedure had the form $V_r = 0.5\,K_r(r_c - r_0)^2$, where K_r is the force constant and r_0 is the reference value of the reaction coordinate. After a 40 ps equilibration with a restraining potential of $K_r = 750$ kJ mol^{-1} Å^{-2} and $r_0 = 0$, the umbrella sampling procedure was started. 24 different values of V_r were used with r_0 values ranging from 0 to ± 3.8 Å and K_r values from 200 to 650 kJ mol^{-1} Å^{-2}. With each V_r, 5 ps were used for equilibration and 20 ps for sampling.

Table 2. Potential energy function parameters and solvent model used in the MD simulations [a].

Atom type	C_{12} (10^7 kcal mol^{-1} Å^{12})	C_6 (kcal mol^{-1} Å^6)	Charge (e)
solute Cl	2.5553	3299.4	–
solute N	0.040450	582.26	–
solute H	0.0	0.0	–
solvent CH_3 [b]	0.62500	2121.5	0.18
solvent O	0.017724	540.56	−0.36

[a] The Lennard-Jones interactions take the form $V_{ij} = C_{12}^{ij}/r_{ij}^{12} - C_6^{ij}/r_{ij}^6$, where r_{ij} is the distance between the two atoms. Combination rules for the parameters are $C_{12}^{ij} = (C_{12}^i C_{12}^j)^{1/2}$ and $C_6^{ij} = (C_6^i C_6^i)^{1/2}$. [b] $r_{C-O} = 1.41$ Å, ∢C-O-C = 111.0°.

Ab initio calculations were carried out with the GAUSSIAN 92 programs [14]. Semiempirical calculations were carried out with the MOPAC programs [15]. MD simulations were carried out with the GROMOS programs [11] and MOPAC modules modified to integrate the quantum-chemical and the force-field methods.

Acknowledgements: We gratefully acknowledge financial support from the Huber–Kudlich Foundation (grant 2-89-100-91).

Received: February 2, 1995 [F157]

[1] a) M. J. Field, P. A. Bash, M. Karplus, *J. Comput. Chem.* **1990**, *11*, 700; b) V. Luzhkov, A. Warshel, *ibid.* **1992**, *13*, 199; c) J. Gao, *J. Phys. Chem.* **1992**, *96*, 537; d) H. Liu, F. Müller-Plathe, W. F. van Gunsteren, *J. Chem. Phys.* **1995**, *102*, 1722.
[2] F. Müller-Plathe, W. F. van Gunsteren, *Macromolecules* **1994**, *27*, 6040.
[3] J. J. P. Stewart, *J. Comput. Chem.* **1989**, *10*, 221.
[4] P. Beak, J. Li, *J. Am. Chem. Soc.* **1991**, *113*, 2796.
[5] M. Bühl, H. F. Schaefer III, *ibid.* **1993**, *115*, 364.
[6] a) J. Chandrasekhar, S. F. Smith, W. L. Jorgensen, *J. Am. Chem. Soc.* **1985**, *107*, 154; b) J. Chandrasekhar, W. L. Jorgensen, *ibid.* **1985**, *107*, 2974; c) W. L. Jorgensen, J. K. Buckner, *J. Phys. Chem.* **1986**, *90*, 4651; d) H.-K. Huang, G. King, S. Creighton, A. Warshel, *J. Am. Chem. Soc.* **1988**, *110*, 5297.
[7] B. D. Wladkowski, W. D. Allen, J. I. Brauman, *J. Phys. Chem.* **1994**, *98*, 13532.
[8] B. D. Wladkowski, K. E. Lim, W. D. Allen, J. I. Brauman, *J. Am. Chem. Soc.* **1992**, *114*, 9136.
[9] S. R. Vande Linde, W. L. Hase, *J. Phys. Chem.* **1990**, *94*, 2778.
[10] G. M. Torrie, J. P. Valleau, *J. Comput. Phys.* **1977**, *23*, 187.
[11] W. F. van Gunsteren, H. J. C. Berendsen, *Groningen Molecular Simulation (GROMOS) Library Manual*, Biomos, Nijenborgh 4, 9747 AG Groningen (The Netherlands).
[12] J.-P. Ryckaert, G. Ciccotti, H. J. C. Berendsen, *J. Comput. Phys.* **1977**, *23*, 327.
[13] H. J. C. Berendsen, J. P. M. Postma, W. F. van Gunsteren, A. DiNola, J. R. Haak, *J. Chem. Phys.* **1984**, *81*, 3684.
[14] M. J. Frisch, G. W. Trucks, M. Head-Gordon, P. M. W. Gill, M. W. Wong, J. B. Foresman, B. G. Johnson, H. B. Schlegel, M. A. Robb, E. S. Replogle, R. Gomperts, J. L. Andres, K. Raghavachari, J. S. Binkley, C. Gonzalez, R. L. Martin, D. J. Fox, D. J. Defrees, J. Baker, J. J. P. Stewart, J. A. Pople, *Gaussian 92, Revision B*, Gaussian, Pittsburgh PA, **1992**.
[15] J. J. P. Stewart, *QCPE Program No. 455*.